Effect of Zn substitution on the normal-state magnetoresistivity of epitaxial $Y_{0.95}Ca_{0.05}Ba_2(Cu_{1-x}Zn_x)_3O_y$ and $Y_{0.9}Ca_{0.1}Ba_2Cu_3O_y$ films

I. Kokanović,* J. R. Cooper, S. H. Naqib,† and R. S. Islam†
IRC in Superconductivity and Department of Physics, University of Cambridge, Madingley Road, Cambridge CB3 OHE, United Kingdom

R. A. Chakalov
Physics Department, University of Birmingham, United Kingdom

(Received 13 September 2005; revised manuscript received 17 March 2006; published 5 May 2006)

We report measurements of the in-plane resistivity, magnetoresistivity (MR) and Hall effect of thin films of slightly under and nearly optimally doped $Y_{0.95}Ca_{0.05}Ba_2(Cu_{1-x}Zn_x)_3O_y$ (with $x=0,0.02,0.04$) and overdoped $Y_{0.9}Ca_{0.1}Ba_2Cu_3O_y$. We found that the introduction of Zn as a dopant strongly suppresses the orbital MR in the normal state. Surprisingly it can be fitted to a T^{-4} law at lower temperatures where the resistivity and cotangent of the Hall angle cot θ_H are relatively constant and no longer obey the usual T^1 and T^2 laws, respectively. In other words, in these samples the increase in residual scattering rate produced by Zn has a stronger effect on cot θ_H than on the MR at low T. It seems that this new result requires some modification of well-known theories involving two distinct relaxation processes for transport and Hall currents.

DOI: 10.1103/PhysRevB.73.184509 PACS number(s): 74.25.Fy, 74.40.+k, 74.62.Dh, 74.72.Bk

I. INTRODUCTION

Understanding the normal state properties of cuprate superconductors, including the unusual variation with temperature and hole concentration of the Hall angle and the magnetoresistance (MR) could be an important step towards a correct microscopic theory of cuprate superconductivity. The hole concentration is usually expressed in terms of a parameter p, the number of added holes per CuO_2 plane. Current understanding is that the overdoped region, where the pseudogap (PG) energy scale is zero, occurs when $p>0.19$,[1] although even in this region the normal state transport properties are still anomalous. The optimally doped state where T_c is a maximum is at $p=0.16$.

There have been several theories of cuprate magnetotransport. In Anderson's theory[2] the response of the correlated electron system to a longitudinal electric field differs from the response to the Lorentz force, because the former alters the energy of an elementary excitation, while the latter only alters its transverse momentum. This difference gives rise to two distinct scattering times, τ_{tr} and τ_H governing the in-plane resistivity ρ_{ab} and Hall angle θ_H, respectively.[2–4] τ_H is predicted to obey the law $1/\tau_H=A+BT^2$ where the residual scattering term A increases linearly with Zn content and the coefficient B is constant, in approximate agreement with experimental data.[4] In this theory it is expected that the MR will vary as τ_H^2. Strictly speaking the theory predicts the orbital magnetoconductance, but for the large MR effects studied here, this is very similar to the orbital MR, which is defined experimentally as the difference between the MR values for $J\perp B$ and $J\|B$, where J is the current density and B the magnetic field.

A second approach ascribes the appearance of two relaxation times to the charge-conjugation symmetries of the elementary excitations or quasiparticles[5] (or in other words their electron-hole symmetries). In this theory the Hall current, which corresponds to the difference in electron and hole contributions, has a completely different relaxation time to the transport current which is the sum of electron and hole contributions.

A third, more conventional approach, is based on the idea of a Fermi liquid with well-defined quasiparticles whose relaxation time τ is strongly dependent on their wave vector $\mathbf{k}$.[6–10] This basic idea has been explored by several authors with various degrees of success.[6–11] Such a strong $\mathbf{k}$ dependence is a natural consequence of the nearly antiferromagnetic Fermi liquid (NAFL) model developed by Pines and collaborators.[6] In the NAFL model those parts of the Fermi surface that are spanned by the spin fluctuation wave vector $\mathbf{Q}$ will clearly have a much larger scattering rate, and in the PG region probably a lower quasiparticle weight, than the parts which are not spanned.[6,8] More recently Hussey[11] added a new ingredient, namely regions of the Fermi surface where the scattering is very strong still give a significant contribution to the conductivity, corresponding to the mean free path being equal to the lattice parameter. This model then gives a good account of much magnetotransport data for overdoped cuprates.

In this paper we report a systematic study of the magnetotransport properties of optimally or slightly under doped $Y_{0.95}Ca_{0.05}Ba_2(Cu_{1-x}Zn_x)_3O_y$ (with $x=0,0.02,0.04$) and overdoped $Y_{0.9}Ca_{0.1}Ba_2Cu_3O_y$ thin films. We have measured in-plane resistivity, Hall voltage and angular dependent MR in the temperature range from just above T_c up to 300 K. We find that the introduction of Zn strongly suppresses the normal orbital MR $\Delta\rho_{orb}/\rho$. However because T_c is also suppressed we could still determine the characteristic T dependence of $\Delta\rho_{orb}/\rho$ over a substantial temperature range. One intriguing new result is that $\Delta\rho_{orb}/\rho$ can be fitted to T^{-4} behavior in a temperature region where the Hall angle θ_H is varying much more slowly than T^{-2} because of the strong scattering by Zn.

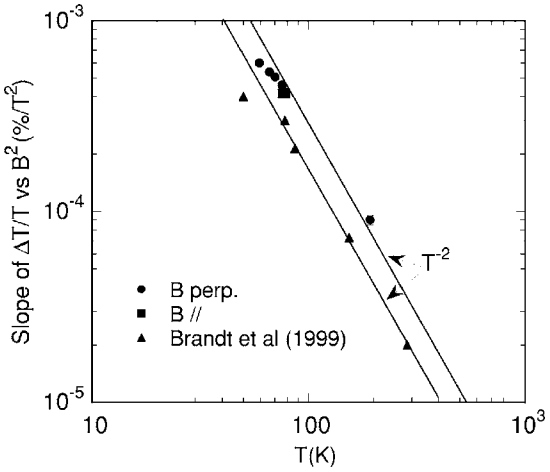

FIG. 1. Comparison of the MR correction for our Cernox thermometer with the average correction for nine thermometers from Ref. 14 (Brandt *et al.*). B perp. or $B\|$ means the applied field was perpendicular or parallel to the axis of the cylindrical thermometer can. In all cases the Cernox MR was negative and the data were fitted to B^2 behavior. In the temperature range of interest 77.8–286 K the slope of the B^2 fit was not changed significantly if some anomalous low-field points in the data of Ref. 14 were omitted, except at 286 K where only points between 14 and 20 T were included in the B^2 fit.

II. EXPERIMENTAL DETAILS

The films were grown on $SrTiO_3$ (100) substrates using pulsed laser deposition. Details of the method can be found in Refs. 12 and 13. Film stoichiometry was determined by electron probe microanalysis (EPMA) using single crystal $YBa_2Cu_3O_{7-y}$, $CaCO_3$, and ZnO as standards. Atomic force microscopy (AFM) was used to examine the surface quality of the films and to determine their thickness, which is 300±45 nm. The films were patterned into the standard shape shown later in the inset to Fig. 2(b), with two pairs of Hall and MR contacts per sample and silver paint contacts being made to evaporated gold pads. The transport measurements were made using standard low frequency ac methods with a measuring current of 10 μA. MR was measured in two ways (i) by sweeping the magnetic field from zero to 11 T and back, and (ii) by rotating the sample from 0° to 285° and back in a fixed magnetic field (usually 11 T) at constant temperature. In the former case the temperature was controlled to better than 5 mK using a Cernox thermometer mounted on the rotatable sample stage. For the latter, a RhFe thermometer whose orientation was fixed, was used to stabilize the temperature as the sample stage was rotated. The Cernox resistance sensor was carefully calibrated in magnetic fields up to 11 T with constant (or slowly drifting) temperatures provided by liquid nitrogen held at various pressures using a manostat or by solid CO_2. Figure 1 shows a comparison of our data with published work[14] that gives the average magnetoresistance of nine Cernox sensors. We found that over a large temperature region the temperature correction $\Delta T/T$ varies as $(B/T)^2$. The Cernox MR is a small but important effect, $\Delta T/T/B^2 = 7.1\times10^{-5}$ %/Tesla^2 at 200 K in Fig. 1 giving a correction of 17 mK at 11 T. The standard deviation in the published data[14] for nine sensors is $\sim\pm50\%$ and the results in Fig. 1 for our sensor are well within this. The error bars in MR are estimated at $\pm2\ 10^{-5}$ in $\Delta R/R$ at 11 T, and probably arise mainly from drifts in the gain of the two lock-in amplifiers since the two pairs of voltage contacts often gave different results at this level.

Hall measurements were made by rotating the sample by 180° in a 6 T magnetic field, with linearity checks being made at several temperatures in fields up to 11 T. Because of the strong hole concentration dependence of normal and superconducting properties,[7,8] it is important to determine p as accurately as possible. We have estimated p from room-temperature thermopower, S(290 K), using the correlation of Obertelli *et al.*,[15] expressed numerically[16] as $S(290\ \mathrm{K}) = -139p + 24.2\ \mu\mathrm{V/K}$, for $p > 0.155$, and $S(290\ \mathrm{K}) = 992\exp(-38.1p)\ \mu\mathrm{V/K}$, for $0.05 < p < 0.155$. These values of p are given in Table I together with T_c values and transition widths (FWHM in $d\rho/dT$). For YBCO S(290 K) does not vary much with Zn content[17] so it is still a good measure of p even in the presence of strong in-plane scattering by Zn.

III. RESULTS AND DISCUSSION

The resistivity data of the four thin films are shown in Fig. 2(a) and their properties are summarized in Table I. From previous work[18] the lower values of p correspond to a pseudogap value of $T^* = 200\pm10$ K. Hence the downturn in resistivity near 200 K for the 5% Ca 0% Zn sample in Fig. 2(a) is ascribed to the PG. There are no detectable downturns in the resistivity data for the two Zn doped samples. This is consistent with previous work[19,20] and the p values in Table I. Namely the 2% Zn sample has a higher value of p and hence $T^* \sim 100$ K while 3% Zn or more is enough to mask the effect of the PG for $T^* \sim 200$ K. Although there are small variations in p for the $Y_{0.95}Ca_{0.05}Ba_2(Cu_{1-x}Zn_x)_3O_y$ samples shown in Fig. 2(a) and Table I, our results

TABLE I. Summary of results for all samples.

Sample Ca, Zn	T_c (K)	ΔT_c (K)	S(290) (μV/K)	p (holes/Cu)	e (10^4 K^4)
0.05	84.8	0.8	5.6±0.5	0.136±0.002	17.9±1.8
0.05, 0.02	66.0	1.5	2.4±0.5	0.157±0.004	5.5±0.5
0.05, 0.04	33.9	1.1	5.4±0.5	0.137±0.002	1.4±0.14
0.1	79.5	0.7	−5.3±0.5	0.212±0.004	12.3±1.2

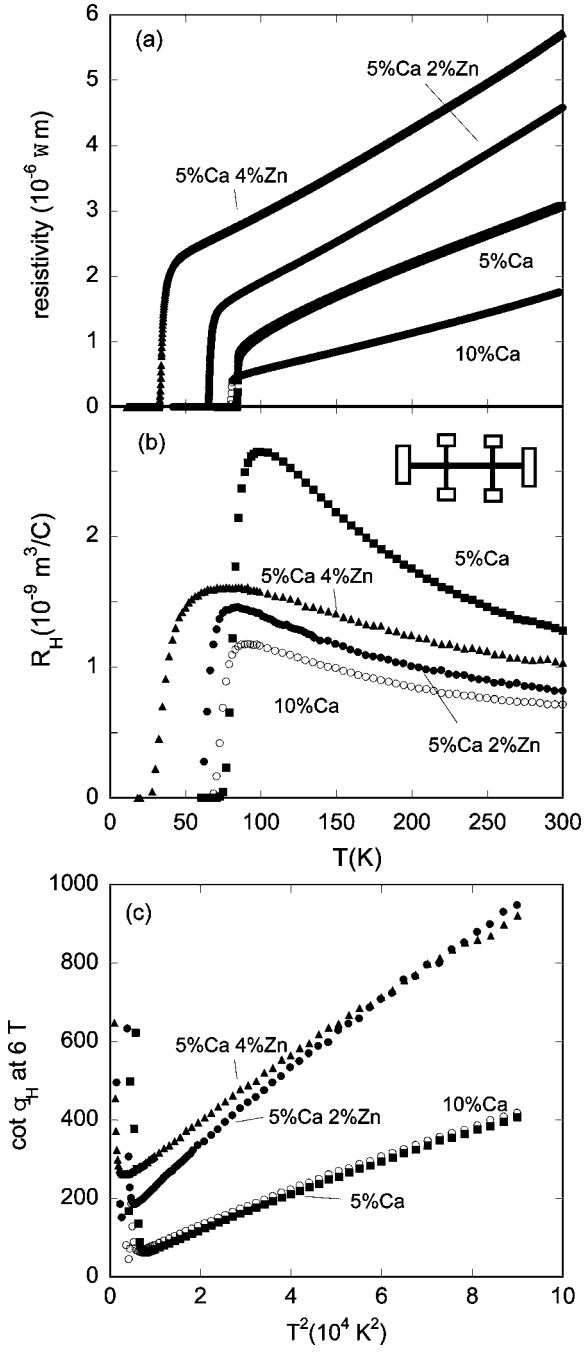

FIG. 2. (a) In-plane resistivity versus temperature for $Y_{0.95}Ca_{0.05}Ba_2(Cu_{1-x}Zn_x)_3O_y$ $(x=0,0.02,0.04)$ and $Y_{0.9}Ca_{0.1}Ba_2Cu_3O_7$ thin films. (b) In-plane Hall coefficient R, for these films. The inset shows a diagram of the patterned films. (c) The corresponding cotangent of the Hall angle, measured at 6 T.

are consistent with an extrapolated residual resistivity, $d\rho_{res}/dx=21\pm2$ $\mu\Omega$ cm/% Zn as obtained previously.[13,18,19] In the present case the oxygen disorder in the Cu-O chains is greater than for Ca-free films, so this residual resistivity definitely represents that from the CuO_2 planes. It is noteworthy that the resistivity of the Zn-free 10% Ca sample ($p=0.212\pm0.004$) is nearly a factor of two lower than the Zn-free 5% Ca one at all T, in agreement with the well-known empirical law[8] that $1/\rho\alpha p$. As is usually found for overdoped

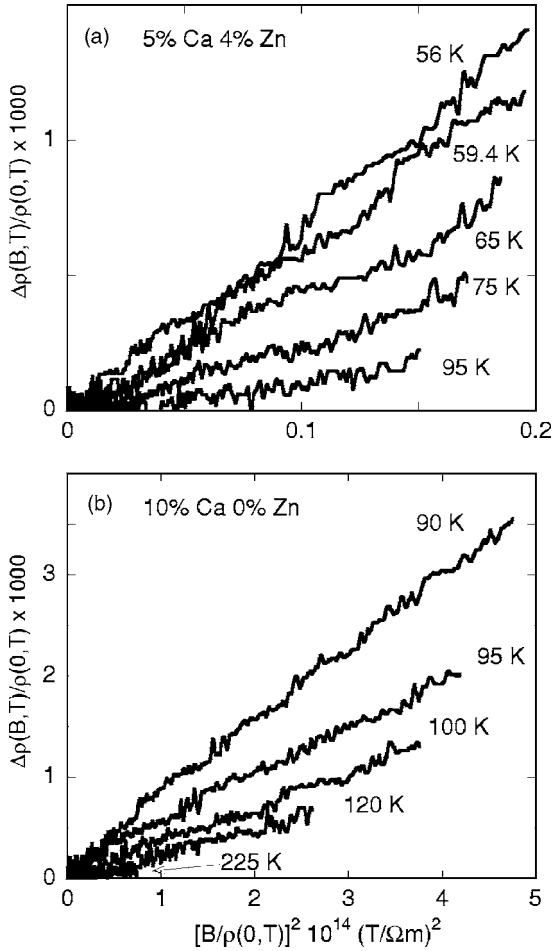

FIG. 3. (a) Kohler plots for the $Y_{0.95}Ca_{0.05}Ba_2$ $(Cu_{0.96}Zn_{0.04})_3O_y$ and (b) $Y_{0.9}Ca_{0.1}Ba_2Cu_3O_7$ thin films.

samples, its T dependence is faster than linear. The 2% and 4% Zn samples have 55% and 60% larger slopes $d\rho(T)/dT$ near 300 K than the 5% Ca, 0% Zn sample, showing that Matthiessen's rule is not exactly obeyed. A similar effect was also observed in a more detailed study of Ca-free films[8,19,20] and for single crystals.[4]

Corresponding Hall coefficient (R_H) data are shown in Fig. 2(b). From previous work[4,7,19] the magnitude of R_H is affected much more strongly by changes in oxygen deficiency than by changes in Zn content. The primary effect of Zn substitution is to suppress the temperature dependence of R_H. A more detailed study of Ca-free films[19] showed that R_H is independent of Zn doping at high T. Our results for the 0 and 4% Zn samples are consistent with this within the uncertainty in film thickness, while R_H values for the 2% Zn sample are lower because p is higher. The 4% Zn data in particular suggest that the broad peak in R_H near 80 K is unlikely to be caused by superconducting fluctuations, since T_c is only 34 K. We believe it arises from the behavior of $\rho(T)$ and θ_H in the normal state. The experimental data for cot $\theta_H \equiv \rho(T)/r_H(T)$ where $r_H \equiv R_H B$ is the Hall resistivity at a field of 6 T and ρ is the in-plane resistivity, respectively, are plotted versus T^2 in Fig. 2(c). The data are approximately linear on this plot with a finite intercept that increases with Zn concentration, as found previously.[4] We see that cot θ_H of

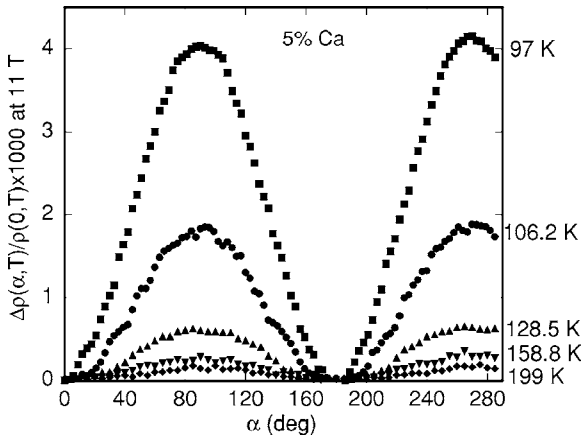

FIG. 4. Angular dependence of the MR for the $Y_{0.95}Ca_{0.05}Ba_2Cu_3O_y$ thin films, α is the angle between the magnetic field and the *ab* plane. $\alpha=0$ corresponds to $B\|J\|ab$ and $\alpha=90$ to $B\|c, J\|ab$.

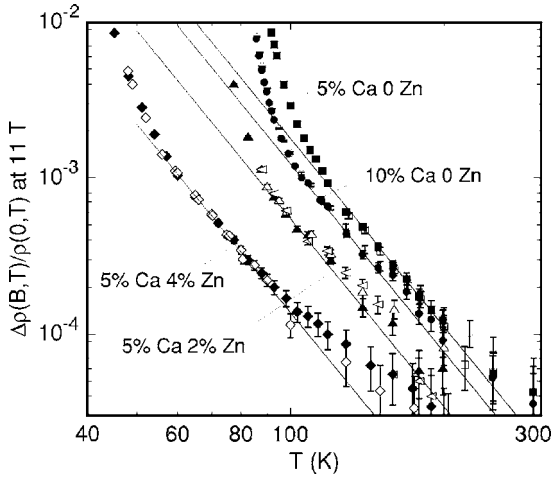

FIG. 5. Log-log plots of the MR in a magnetic field of 11 T for all films studied. Closed symbols orbital part from angular sweeps. Open symbols, total transverse MR from field sweeps. Solid lines show T^{-4} behavior.

the Zn-free samples is also independent of Ca content, i.e. p as also found earlier.[22] There are in fact the same kind of deviations from an $A+BT^2$ law found previously.[4,19,21,22] Namely there is a weak negative curvature for all samples and if the data are fitted to an $A+BT^m$ law over the whole range of T then for all the samples $m=1.67\pm0.03$ rather than $m=2$.

Figures 3(a) and 3(b) show the magnetic field dependence of the in-plane resistivity in transverse geometry ($B\|c, J\perp c$) for the 5% Ca, 4% Zn, and the 10% Ca sample in the form of Kohler plots, namely $\Delta\rho/\rho$ versus $[B/\rho(B=0)]^2$ at several fixed temperatures. The transverse MR is positive and proportional to B^2 from approximately T_c+20 K to 300 K. At temperatures closer to T_c (not shown) the MR starts to show negative curvature on a B^2 plot and would eventually saturate at high fields. This is caused by a decrease in the characteristic magnetic field needed to suppress superconducting fluctuations, which varies as $B_{c2}(T/T_c)$. Well above T_c this characteristic field is of order $B_{c2}(0)$ or 100 T, but at a few degrees both above and below T_c it is only a few Teslas, since just below T_c, $dB_{c2}/dT\sim-2$ T/K.

In conventional metals $\Delta\rho/\rho$ usually varies as $(\omega\tau)^2$, where ω is the cyclotron frequency and τ is the relaxation time, and therefore Kohler's rule $\Delta\rho/\rho\sim(B/\rho)^2$ is obeyed. However, other measurements of YBCO (with various dopings) strongly violate Kohler's rule,[3] so it is not surprising that this also happens for the present samples, indicating that the **k** independent τ approximation never applies. The longitudinal MR ($J\|B, J\perp c$) is also positive but is always much smaller than the transverse MR. It falls below our measurement resolution above approximately T_c+20 K for 5% Ca, 0% Zn, and T_c+50 K for 5% Ca, 4% Zn. For this Zn-doped sample it probably arises from the effect of the magnetic field on the pseudogap, i.e., it is a spin effect, as suggested previously by others.[23] For the Zn-free 5% Ca sample the longitudinal MR probably arises from a combination of this effect and superconducting fluctuations. MR measurements as a function of the angle (α) between magnetic field and the *a-b* plane of the sample have also been performed by rotating the sample at fixed magnetic field and fixed temperatures as described above. Some examples for one of the samples at 11 T are shown in Fig. 4. Similar results were also obtained for the other samples. The angular sweeps could be fitted by $\Delta R/R_0=m_1\alpha+m_2\sin\alpha+m_3\sin^2\alpha$ where m_1 represents a linear temperature drift term, m_2 is a T dependent Hall contribution linear in magnetic field, and m_3 is the orbital MR which generally dominates, scales precisely as B^2 and falls rapidly with increasing temperature. Thus, m_3 allows separation of the orbital MR from the total MR. Data for all samples are shown as log-log plots of $\Delta\rho(B,T)/\rho(0,T)$ versus T, with $B=11$ T in Fig. 5. The data shown include those from (a) field sweeps in which the data were fitted to $\Delta\rho(B,T)/\rho(0,T)=dB^2$ (open symbols), this gives the total transverse MR including orbital and spin parts, or (b) angle sweeps, (closed symbols), which give the orbital MR. The close correspondence between the two types of data underlines the smallness of the isotropic (spin) part mentioned above. The solid lines represent the power law $\Delta\rho(B,T)/\rho(0,T)=eT^{-4}$, and the values of e are given in Table I. Because of the resolution limit mentioned previously the orbital MR can be detected up to 300 K for $x=0$, but only up to 200 K and 160 K for Zn contents $x=0.02$ and $x=0.04$, respectively. The strong T^{-4} dependence of $\Delta\rho(B,T)/\rho(0,T)$, while $\rho(0,T)\simeq a+bT+cT^2$, corresponds to the strong deviations from Kohler's rule shown in Fig. 3.

Although a Fermi liquid model may not apply to the cuprates,[2,5] for a two-dimensional (2D) Fermi liquid the orbital MR arises from the variance of the local Hall angle around the Fermi surface[3] and can be written as

$$\Delta\rho(B,T)/\rho(T)=\langle\theta(s)^2\rangle-\langle\theta(s)\rangle^2, \quad (1)$$

where $\langle A\rangle\equiv\oint A(s)\Sigma(s)ds/\oint\Sigma(s)ds$, $\Sigma(s)$ is the conductivity and ds is an element of length along the Fermi surface. $\theta(s)$ is the local Hall angle and is proportional to $\tau(s)$ the relaxation time in the elemental length ds multiplied by a local curvature factor related to the effective mass. In the earlier

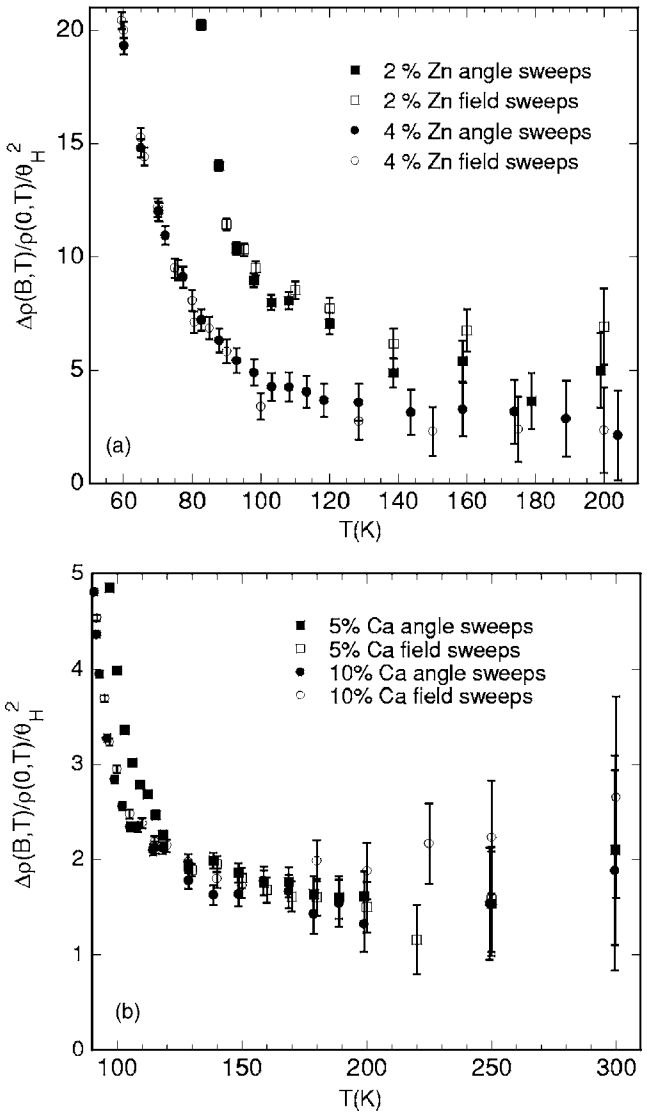

FIG. 6. The ratio of the MR to the square of the Hall angle for all films studied.

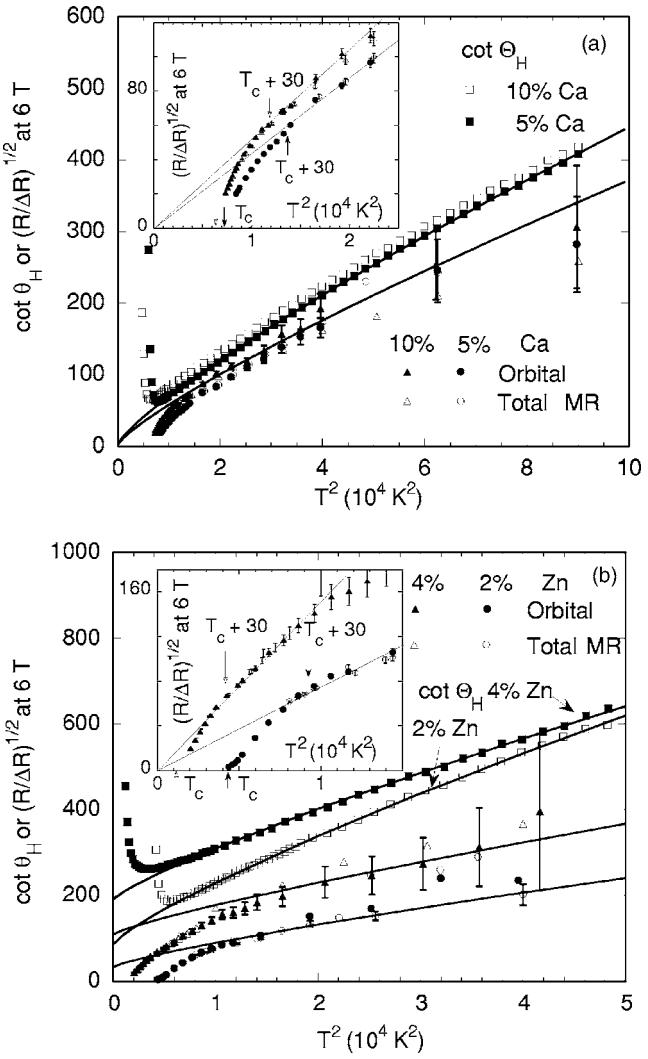

FIG. 7. Direct comparison of MR and Hall angle data, both at 6 T for the four films studied in the form of $(R/\Delta R)^{1/2}$ and cot θ_H vs T^2 plots. The solid lines are fits to a power law cot $\theta_H = A + BT^m$, with $m = 1.65$. The same fits have been multiplied by factors of 0.5 to 0.8 for comparison with the corresponding MR data. The inserts show the low T region where the limiting T^{-4} behavior and the onset of fluctuations are visible.

work[3] on pure YBCO the observation that $\Delta\rho(B,T)/\rho(T) \sim T^{-4}$ while $\langle\theta(s)\rangle^2 \sim T^{-4}$ was used to rule out the Fermi liquid model with a **k** dependent τ. Namely in the simplest version of such models the variance in τ, $[\langle\tau(s)^2\rangle - \langle\tau(s)\rangle^2]/\langle\tau(s)\rangle^2$ has to be strongly T dependent in order to account for the T dependence of R_H which is enhanced by a factor $\overline{\tau(s)^2}/[\overline{\tau(s)}]^2$, where in this formula $\overline{\tau(s)}$ is the mean value of $\tau(s)$ without any conductivity weighting factor $\Sigma(s)$.[24] But this is difficult to reconcile with Eq. (1), if $\Delta\rho/\rho$ and $\langle\theta\rangle^2$, i.e., $\langle\tau(s)\rangle^2$ have the same T dependences. However the anisotropic $\tau(\mathbf{k})$ model proposed by Hussey[11] does give agreement with the behavior of the Hall angle and MR within experimental error. This is presumably because in this model the regions of the Fermi surface (FS) where $\tau(s) \sim T^{-2}$ dominate both the Hall angle and MR. In the other regions the mean free path is equal to the in-plane lattice parameter and is therefore small and T independent. Furthermore the argument of Ref. 3 will not hold if the effective mass varies with temperature, for example from renormalization effects in a correlated electron system, and probably even if it varies very strongly around the Fermi surface. In the present work we find that the relation between the MR and the Hall angle is not the same at higher and lower temperatures, as discussed in more detail later.

Since the values of T_c of the various samples range between 85 and 34 K, superconducting fluctuations will affect the $\Delta\rho(B,T)/\rho(T)$ curves quite differently. The data in Fig. 5 suggest that superconducting fluctuations only become important below T_c+30 K, where there are strong upward deviations from the T^{-4} lines. The data suggest that the onset of fluctuations is relatively rapid below this temperature. In combination with appropriate theory these data could be used to shed light on another topic of current interest, namely the mechanism by which the fluctuation contributions to various physical properties is cut off above T_c. For Bi:2212 crystals the MR has been ascribed to superconducting

fluctuations[25] over the whole temperature range (up to 300 K). The present work suggests that the possibility of a T^{-4} term in the MR of Bi:2212 should also be considered, as an alternative to fluctuations, although they are larger in lower-dimensional systems and Bi:2212 is admittedly much more anisotropic than the YBCO samples studied here.

The ratios of the normal orbital MR to the square of the Hall angle, i.e., $[\Delta\rho(B,T)/\rho(T)]/\theta_H^2$ in a field of 11 T are shown for all four samples in Figs. 6(a) and 6(b). It can be seen that in the Zn-free samples the ratios are 2 ± 0.2 at 120 K, and decrease weakly with increasing temperature, i.e., they are consistent with the law $[\Delta\rho(B,T)/\rho(T)]\sim\theta_H^2$. On the other hand, for the Zn-doped samples the ratios are larger and more T dependent, increasing to values as high as 20 at 60 K ($x=0.04$). Thus, the observed normal orbital MR for these samples is only comparable to $\langle\theta(s)\rangle^2$ (within a factor two) at higher temperatures, above approximately 130 K. In LSCO the ratio $[\Delta\rho(B,T)/\rho(T)]/\theta_H^2$ is also much larger[3,26] and only T independent for certain values of p.[26] Similar results were found for c axis oriented epitaxial Bi-2212 films.[27]

Although the plots in Fig. 6 do show large differences between the MR and inverse Hall angle at low T, they are slightly misleading in that the main difference occurs in the residual term A rather than the BT^2 term. In our opinion the combined plots of $(R/\Delta R)^{1/2}$ and cot θ_H vs T^2 shown in Fig. 7 are more revealing. At higher values of T both quantities have similar slopes, the main difference, especially for the Zn doped samples, is that the low T intercept A is larger for cot θ_H than for $(R/\Delta R)^{1/2}$. Furthermore, below $\sim$100 K the intercept of $(R/\Delta R)^{1/2}$ disappears quite abruptly and as shown in the insets, the data can be fitted to T^{-4} laws, which is consistent with the conclusions drawn from the log-log plots in Fig. 5. The insets to Fig. 7 also show how superconducting fluctuations become significant below T_c+20 to T_c+30 K as well as the expected divergence in $\Delta R/R$ as $T\rightarrow T_c$, i.e., $(R/\Delta R)^{1/2}$ extrapolates to zero near T_c. Therefore, from the plots shown in Fig. 7 we can see that the two-lifetime pictures work reasonably well at higher T although, even there, Zn substitution does have a significantly larger effect on the residual scattering term in cot Θ_H than that in $(R/\Delta R)^{1/2}$. At lower temperatures this effect becomes even more extreme in that the MR can be fitted to a T^{-4} law with no significant residual scattering term, while the residual term in cot Θ_H remains finite, although probably smaller than that at higher T. Within the **k** dependent τ model of Hussey[11] one possibility is that these unusual effects arise because of anisotropic **k** dependent scattering by Zn atoms.[28] This is currently being investigated numerically. Anisotropic scattering by zinc atoms might be a possible way of accounting for the discrepancies between our data and the non-Fermi liquid two-lifetime models at low T.

IV. SUMMARY AND CONCLUSIONS

In summary, we report measurements of the in-plane resistivity, magnetoresistivity, and Hall resistivity of under and nearly optimally doped $Y_{0.95}Ca_{0.05}Ba_2(Cu_{1-x}Zn_x)_3O_y$ ($x=0,0.02,0.04$) and overdoped $Y_{0.9}Ca_{0.1}Ba_2Cu_3O_7$ films. The orbital MR is strongly suppressed with increasing Zn concentration, but the lower T_c values have allowed us to follow its T dependence over a substantial temperature range. There are deviations from the two-lifetime models in that at low T the extra scattering introduced by zinc doping has a stronger effect on cot Θ_H than it does on the orbital MR which can still be fitted to a T^{-4} law.

ACKNOWLEDGMENTS

We are grateful to John Loram for useful discussions, to John Durrell for help in patterning the films, to Chris Hayward for electron microprobe analysis, and to Ahmed Kuršumović for atomic force microscopy. This work was supported by EPSRC (UK), Grant No. EP/C511778/1 and the Croatian Research Council.

*Corresponding author. Email address: kivan@phy.hr. On leave from Department of Physics, Faculty of Science, University of Zagreb, P.O. Box 331, Zagreb, Croatia.

†Present address: Department of Physics, University of Rajshahi, 6205, Bangladesh.

[1] J. W. Loram, K. A. Mirza, J. R. Cooper, and J. L. Tallon, J. Phys. Chem. Solids **59**, 2091 (1998).

[2] P. W. Anderson, Phys. Rev. Lett. **67**, 2092 (1991).

[3] J. M. Harris, Y. F. Yan, P. Matl, N. P. Ong, P. W. Anderson, T. Kimura, and K. Kitazawa, Phys. Rev. Lett. **75**, 1391 (1995).

[4] T. R. Chien, Z. Z. Wang, and N. P. Ong, Phys. Rev. Lett. **67**, 2088 (1991).

[5] P. Coleman, A. J. Schofield, and A. M. Tsvelik, Phys. Rev. Lett. **76**, 1324 (1996).

[6] B. P. Stojkovic and D. Pines, Phys. Rev. Lett. **76**, 811 (1996).

[7] A. Carrington, A. P. Mackenzie, C. T. Lin, and J. R. Cooper, Phys. Rev. Lett. **69**, 2855 (1992).

[8] J. R. Cooper and J. W. Loram, J. Phys. I **6**, 2237 (1996).

[9] R. Hlubina and T. M. Rice, Phys. Rev. B **51**, 9253 (1995).

[10] L. B. Ioffe and A. J. Millis, Phys. Rev. B **58**, 11631 (1998).

[11] N. E. Hussey, Eur. Phys. J. B **31**, 495 (2003).

[12] S. H. Naqib, Ph.D. thesis, University of Cambridge, 2003.

[13] S. H. Naqib, J. R. Cooper, J. L. Tallon, R. S. Islam, and R. A. Chakalov, Phys. Rev. B **71**, 054502 (2005).

[14] B. L. Brandt, D. W. Liu, and L. G. Rubin, Rev. Sci. Instrum. **70**, 104 (1999).

[15] S. D. Obertelli, J. R. Cooper, and J. L. Tallon, Phys. Rev. B **46**, R14928 (1992).

[16] J. L. Tallon, C. Bernhard, H. Shaked, R. L. Hitterman, and J. D. Jorgensen, Phys. Rev. B **51**, R12911 (1995).

[17] J. L. Tallon, J. R. Cooper, P. S. I. P. N. deSilva, G. V. M. Williams, and J. W. Loram, Phys. Rev. Lett. **75**, 4114 (1995).

[18] S. H. Naqib, J. R. Cooper, J. L. Tallon, and C. Panagopoulos, Physica C **387**, 365 (2003).

[19] D. J. C. Walker, A. P. Mackenzie, and J. R. Cooper, Physica C **235–240**, 1335 (1994).
[20] D. J. C. Walker, A. P. Mackenzie, and J. R. Cooper, Phys. Rev. B **51**, R15653 (1995).
[21] A. Carrington, D. J. C. Walker, A. P. Mackenzie, and J. R. Cooper, Phys. Rev. B **48**, 13051 (1993).
[22] I. R. Fisher, Ph.D. thesis, University of Cambridge, 1996.
[23] Y. Ando and K. Segawa, Phys. Rev. Lett. **88**, 167005 (2002).
[24] *The Hall Effect in Metals and Alloys*, edited by C. M. Hurd (Plenum Press, New York-London, 1972), p. 75.
[25] Yu. I. Latyshev, O. Laborde, and P. Monceau, Physica C **235–240**, 1525 (1994).
[26] F. F. Balakirev, I. E. Trofimov, S. Guha, M. Z. Cieplak, and P. Lindenfeld, Phys. Rev. B **57**, R8083 (1998).
[27] Z. Konstantinovic, O. Laborde, P. Monceau, Z. Z. Li, and H. Raffy, Physica B **259–261**, 569 (1999).
[28] N. E. Hussey (private communication).